A nonneural miRNA cluster mediates hearing via repression of two neural targets

Binglong Zhang, Hong Duan, Joshua Kavaler, Lu Wei, Daniel F. Eberl, and Eric C. Lai

¹Developmental Biology Program, Sloan Kettering Institute, New York, New York 10065, USA; ²Department of Biology, Colby College, Waterville, Maine 04901, USA; ³Department of Biology, University of Iowa, Iowa City, Iowa 52242, USA

We show here that *mir-279/996* are absolutely essential for development and function of Johnston's organ (JO), the primary proprioceptive and auditory organ in *Drosophila*. Their deletion results in highly aberrant cell fate determination, including loss of scolopale cells and ectopic neurons, and mutants are electrophysiologically deaf. In vivo activity sensors and mosaic analyses indicate that these seed-related miRNAs function autonomously to suppress neural fate in nonneuronal cells. Finally, genetic interactions pinpoint two neural targets (*elav* and *insensible*) that underlie miRNA mutant JO phenotypes. This work uncovers how critical post-transcriptional regulation of specific miRNA targets governs cell specification and function of the auditory system.

[Keywords: Drosophila; Johnston's organ; hearing; microRNA; neuron]

Supplemental material is available for this article.

Received August 7, 2023; revised version accepted November 29, 2023.

Hearing is one of the fundamental sensory modalities that allows animals to interpret the world at large. Indeed, hearing impairment is the most common sensory deficit in humans (Hildebrand et al. 2008), with one in eight people in the United States over age 12 showing significant hearing loss in both ears (Lin et al. 2011). In insects, sound is detected by chordotonal organs, mechanosensitive stretch receptors that collectively detect long-range acoustic waves or short-range vibrations; each is a multicellular structure termed a scolopidium (Boekhoff-Falk and Eberl 2014; Jarman 2014). In Diptera, numerous scolopidia are arrayed within the Johnston's organ (JO), an antennal structure responsible for sensing sound (Eberl et al. 2000), gravity (Armstrong et al. 2006; Kamikouchi et al. 2009), and wind (Yorozu et al. 2009). The JO is the largest mechanosensory organ in many insects. For example, the JOs of male Aedes aegypti harbor ~7000 scolopidia (Boo and Richards 1975), many more than the ~800 light-sensing ommatidial units in each eye (Singh and Mohan 2013).

The insect JO is analogous to the mammalian inner ear, and these organs exhibit similar development (Todi et al. 2005; Eberl and Boekhoff-Falk 2007; Jarman and Groves 2013; Fritzsch et al. 2020) and function (Caldwell and Eberl 2002; Albert et al. 2007; Kavlie and Albert 2013; Christie and Eberl 2014). While hearing can be damaged by prolonged exposure to loud sounds, there is now a rich foundation to understand the genetic basis of functional audition (Petit 2006; Dror and Avraham 2009). Ac-

Corresponding author: laie@mskcc.org

Article published online ahead of print. Article and publication date are online at http://www.genesdev.org/cgi/doi/10.1101/gad.351052.123.

cordingly, the powerful genetics of an insect model such as *Drosophila melanogaster* makes it a compelling system to discover fundamental principles of the auditory system (Albert et al. 2007, 2020; Li et al. 2018). These range from high-level transcriptional regulators such as proneural bHLH factors (Jarman et al. 1993; Bermingham et al. 1999; Cachero et al. 2011) and Notch target genes (Zine et al. 2001) to loci involved in differentiation and morphogenesis, such as *crinkled/myosinVIIA* (Todi et al. 2008) and *diaphanous* (Lynch et al. 1997; Schoen et al. 2010).

Drosophila JOs are contained in the second antennal segment and consist of ~225 scolopidia (Fig. 1A; Boekhoff-Falk and Eberl 2014; Jarman 2014). Similar to other peripheral sense organs (Lai and Orgogozo 2004), each of these chordotonal organs derives from an individual precursor cell, which undergoes a stereotyped lineage involving multiple asymmetric divisions to yield the distinctive complement of neurons and supporting cells that comprise a functional organ (Fig. 1B). JOs bear ~480 total sensory neurons (Kamikouchi et al. 2006), implying that each scolopidium contains about two neurons. In fact, >10% of JO scolopidia contain three dendrites (Todi et al. 2004), and such triply innervated sensory organs may explain the slight excess of neurons to scolopidia across the entire JO. Until now, the details of the cell lineage(s) in JO scolopidia have not been fully known, and antibodies that distinguish the neural subtypes have not been described.

© 2023 Zhang et al. This article is distributed exclusively by Cold Spring Harbor Laboratory Press for the first six months after the full-issue publication date [see http://genesdev.cshlp.org/site/misc/terms.xhtml]. After six months, it is available under a Creative Commons License [Attribution-NonCommercial 4.0 International], as described at http://creativecommons.org/licenses/by-nc/4.0/.

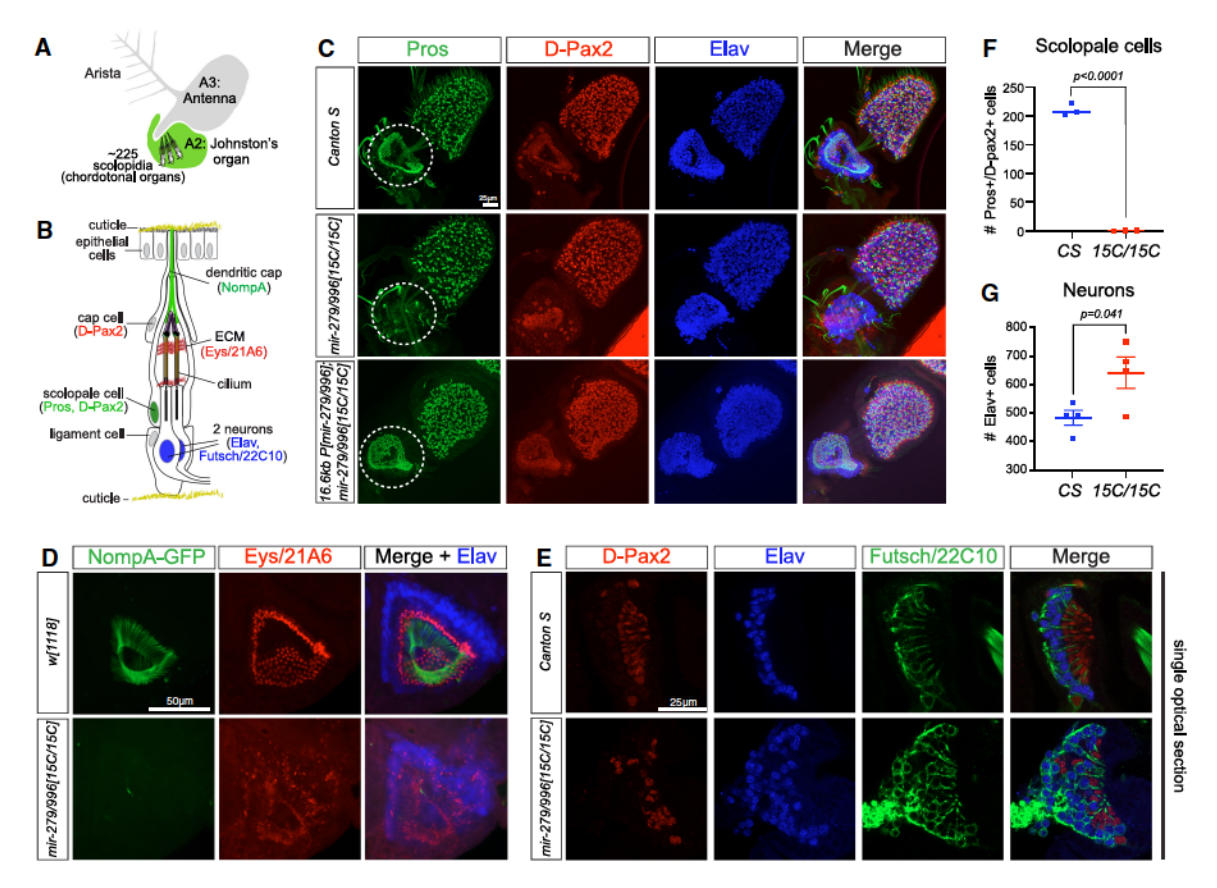


Figure 1. mir-279/996 are essential for appropriate cell fate in Johnston's organs. (A,B) Cellular organization of the antenna, Johnston's organ, and scolopidium. (A) The Drosophila antenna is segmented, with the largest regions comprising A3 (decorated with olfactory sensilla) and A2 (bearing the Johnston's organ [JO]). JOs house ~225 chordotonal organs, termed scolopidia, which are arrayed radially and converge on the focal joint between A2 and A3 to detect rotation of A3. (B) Schematic of cells and structures in an individual scolopidium. These multicellular stretch receptors are anchored on both ends to the cuticle, with the epithelial cell layer oriented on the apical side at the joint with A3. The differentiated scolopidial cell types and characteristic markers are labeled. Nuclear fate markers are indicated on their respective cell types. Markers of differentiated cells include NompA-GFP (secreted by scolopale cells and integrated into the dendritic cap) and 21A6/Eys (a neuronal product deposited in the ECM of the scolopale space). (C) Whole antennae at 45 h after puparium formation (APF), stained for scolopale (Pros) and neuronal (Elav) markers. The JO is marked by a dotted circle, and its stereotyped organization is exemplified by wild-type Canton S (CS). The A2/JO is selectively ablated in mir-279/996/15Cl-null mutants, but A3 olfactory sensilla maintain relatively normal expression of fate markers. The miRNA mutants lose most high-Pros nuclei, although cells with low-Pros remain. The mir-279/996[15C] JO is fully rescued by a 16.6-kb mir-279/996 genomic transgene. (D,E) Analysis of differentiation markers 21A6/Eys and NompA-GFP confirmed that scolopale cells selectively fail to mature in mir-279/996[15C] (D) and that Elav⁺ neurons elaborate processes that label with 22C10/Futsch (E). Note that all these markers exhibit characteristic normal patterns in control genotypes w[1118] and Canton S; only one control is shown in these panels. (F,G) Quantification of scolopale cells (F) and neurons (G) in control CS and mir-279/996[15C] deletion mutants. At least three JO samples were analyzed per genotype, and each dot quantifies cell markers in all the scolopidia from each individual in a 3D volume. Statistical significance was evaluated using unpaired t-tests.

However, based on the inferred differential expression of certain neuronal Gal4 lines in JOs, it was proposed that they are often heteromorphic; i.e., combining an auditory neuron and a wind/gravity-sensing neuron (Ishikawa et al. 2019).

The proper assignment and execution of neural and nonneural cell fates depends on intrinsic regulators (e.g., cell-specific transcription factors) and cell-cell signaling between sibling daughter cells via the Notch pathway. In particular, Notch signaling diverts daughter cells in peripheral sensory organ lineages from the neural fate and further differentiates them from each other, yielding scolopale, ligament, and cap cells (Fig. 1B). A striking mani-

festation of the requirement for Notch signaling for asymmetric divisions is the fact that genetic manipulation of this pathway induces symmetric fate outcomes in many types of sensory organs (Hartenstein and Posakony 1990; Lai 2004). Moreover, these can be predictably biased in either direction, depending on whether Notch signaling is inhibited or ectopically activated. However, while the role of Notch in asymmetric division in neural lineages has been extensively studied, it has not received attention within the JO scolopidial lineage to date.

Transcription factors (TFs) and chromatin factors are the best-studied regulators of cell fate, but post-transcriptional regulation by RNA binding proteins (RBPs) and microRNAs (miRNAs) can have strong consequences on gene expression and cell state. At the same time, numerous RBPs remain to be functionally characterized (https ://bio.tools/EuRBPDB), and it is also recognized that most knockouts of well-conserved miRNAs do not grossly perturb development or physiology (Alvarez-Saavedra and Horvitz 2010; Park et al. 2012; Chen et al. 2014). Thus, despite systematic efforts to collect certain functional attributes of RBPs and miRNAs (Ray et al. 2013; Agarwal et al. 2015; Van Nostrand et al. 2020), we know far less about how these post-transcriptional regulators affect in vivo biology compared with TFs and chromatin factors. Nevertheless, RNA-mediated regulation is critical for development and/or function of the inner ear (Avraham et al. 2022; Shi et al. 2022). For example, recent studies demonstrate that mutations of RBPs such as Caprin1 (Nolan et al. 2022), Lin28B (Li et al. 2022), and SRRM4 (Nakano et al. 2020) are all deleterious in this setting. Moreover, mammalian mir-96 and its clustered paralogs, mir-183 and mir-182, were some of the first miRNAs known to be specifically expressed in ciliated sensory organs, including the inner ear (Pierce et al. 2008), and to be genetically required for its development and for functional hearing (Lewis et al. 2009, 2020; Kuhn et al. 2011).

In this study, we report that deletion of the clustered paralogs mir-279/996 has profound consequences on cell specification within the Drosophila JO, with a near-complete absence of scolopale cells and a concomitant increase in neurons. As the scolopale and neuron are sister cells, this indicates a failure in Notch-mediated asymmetric division, and this defect results in complete deafness. Although other defects have been documented in mir-279/996 mutants, especially in the nervous system (Cayirlioglu et al. 2008; Luo and Sehgal 2012; Sun et al. 2015; Sanfilippo et al. 2016; Duan et al. 2018; Kavaler et al. 2018), the annihilation of the JO is one of the most profound developmental and behavioral defects known for a miRNA knockout. A recurrent theme in prior studies is that miR-279/996 suppress the neuronal fate in nonneural cells, although curiously, the relevant target genes are often different in different tissues. Here, we found that double heterozygosity of two nuclear, neural-expressed miR-279/996 targets—the Notch inhibitor insensible and the mRNA processing factor *elav*—can fully restore normal JO development and audition to mir-279/996 knockouts. This genetic rescue is particularly striking, as insensible mutants lack substantial PNS defects and Elav is not known to influence cell fate specification. Therefore, genetic analysis of miRNAs leads to new regulatory strategies that underlie the assembly of sensory organs and reception of environmental stimuli.

Results

The mir-279/996 cluster is essential for development of the Johnston's organ (JO)—the fly ear

mir-279/996[15C] deletion animals are extremely poorly coordinated and are prone to dying prematurely in their food, although they can survive some days with very care-

ful culturing (Sun et al. 2015). Since these defects may not be explained well by neural settings studied in previous reports (e.g., the olfactory system, notum bristles, and the eye) (Cayirlioglu et al. 2008; Hartl et al. 2011; Sun et al. 2015; Duan et al. 2018; Kavaler et al. 2018), we considered whether other sensory systems might be affected. Chordotonal organs are a major class of type I sensory organ that provide proprioception and are present in several adult locations, including the legs, wings, abdomen, and antenna. The antennal chordotonal organ, termed the Johnston's organ (JO), is also responsible for hearing (Eberl et al. 2000; Boekhoff-Falk and Eberl 2014) and is analogous to the mammalian inner ear (Lu et al. 2009; Christie and Eberl 2014). Drosophila JOs develop from the second antennal segment (Fig. 1A) and are composed of ~225 scolopidia, each comprising a multicellular chordotonal organ containing two or three neurons and several support cells: the scolopale, cap, and ligament cells (Fig. 1B; Kamikouchi et al. 2006; Ishikawa et al. 2019).

We assayed several JO cell markers at 45 h after pupal formation (APF), when specification and basic morphogenesis of JOs is complete. These included Elay (a canonical neural antigen), Prospero (specific to the scolopale cell), and D-Pax2 (expressed in scolopale and cap cells). Note that to our knowledge, D-Pax2 expression has not been analyzed previously in JOs but is expressed in these cell types in embryonic chordotonal organs (Avetisyan et al. 2021). Because the antenna has 3D architecture and hundreds of scolopidia are packed tightly within JOs, it is difficult to discern cell numbers without laborious imaging and cell quantification through their volume (Kamikouchi et al. 2006). However, these markers are expressed in a relatively normal and spatially organized fashion throughout sensory organs within the A3 antennal segment (mostly containing olfactory organs) in mir-279/996/15C] deletion animals. In contrast, there is a striking and selective disruption of JO organization, including loss of most strongly Pros⁺ cells (Fig. 1C; Supplemental Fig. S1). A small population of weakly Pros+ cells remains, but these are distinguished from scolopale cells (which costain with D-Pax2) and cap cells (which strongly express D-Pax2 only). In addition, staining for phalloidin, which labels actin rods in scolopale cells and cap cells, was highly reduced in [15C] homozygotes (Supplemental Fig. S2A). Phalloidin staining was not fully lost from mutant JOs, potentially indicating incomplete loss of scolopale identity. In any case, this JO defect was fully rescued by a 16.6-kb genomic transgene covering only mir-279/996 (Supplemental Fig. S2A). Overall, there are strong and specific defects in cell fate and differentiation within JO scolopidia.

We used two additional criteria to verify that these strong defects were truly caused solely by loss of miR-279/996. First, we examined other mutant alleles (Sun et al. 2015), ranging from hypomorphic (ex117) to a strong allele (ex36) to a chromosomal deficiency (i.e., null). Homozygous and trans-heterozygous combinations of these comprise an allelic series, which recapitulated strong loss of Pros⁺ and Pros⁺/D-Pax2⁺ double-positive cells in various strong or null combinations and a weaker

phenotype of scolopale cell loss in *ex117* homozygotes (Supplemental Fig. S1). None of these allelic combinations yielded substantial effects on these markers in the antennal segment. Second, we tested whether these profound developmental defects could be rescued. Indeed, both JO organization and Pros⁺ cells were fully restored upon introduction of a 16.6-kb *mir-279/996* genomic transgene that lacks neighboring protein-coding genes (Fig. 1C; Sun et al. 2015). Together, these tests provide clear evidence that miR-279/996 are specifically required for the presence of scolopale cells within the JOs.

We also assessed differentiated cell markers in mir-279/ 996/15C/-null animals. Glial cells (marked by α-Repo) were not affected (Supplemental Fig. S2B). We also analyzed markers relevant to scolopale cell fate and/or function. mAb 21A6 (a-Eyes Shut [Eys]) is expressed from the neuron but is secreted into the scolopale space (Mahato et al. 2018), while NompA-GFP is expressed by scolopale cells and is secreted into the ECM, where it contributes to the dendritic cap (Chung et al. 2001). Both markers were highly reduced in mutants, consistent with loss of differentiated scolopale cells (Fig. 1D). On the other hand, mAb 22C10 (α-Futsch) labeled axons of mature neurons and stained mutant JO robustly (Supplemental Fig. S2C). Since these studies indicated that a particularly overt defect in mir-279/996/15C/-null mutants was the loss of scolopale cells, we compared 21A6/Eys and NompA-GFP staining across a genetic dosage series. Strikingly, five mutant backgrounds ranging from hypomorphic to null all failed to differentiate scolopale cells (Supplemental Fig. S3), attesting to strong dependence of this cell type on miR-279/996 activity.

Single-plane confocal images emphasize that 22C10/ Futsch reactivity encircled all Elav⁺ nuclei (Fig. 1E). Since scolopale cells and neurons are sister cells, these data suggested potential cell fate transformation in mutants. Accordingly, we carefully quantified strongly Elav⁺ cells and observed that their numbers were substantially increased in 15C-null mutants at the expense of Pros⁺/ D-Pax2⁺ scolopale cells (Fig. 1F,G). Indeed, the loss of scolopale cells was relatively similar to the gain of neurons. Overall, we uncovered new developmental defects in mir-279/996 mutants, which are completely penetrant and exceedingly severe among miRNA mutants.

mir-279/996 mutants are completely deaf

mir-279/996 mutants have severe proprioceptive defects and cannot stand (Fig. 2A). In light of their substantial defects in the development of a major chordotonal organ (Fig. 1), we tested their capacity to hear. To do so, we used electrophysiology to assay sound-evoked potentials (SEPs) from the antennal nerve (Fig. 2B; Eberl and Kernan 2011).

Consistent with their cytology defects, we observed that *mir-279/996[15C]*-null animals exhibited complete deafness (Fig. 2C,D) compared with their normal heterozygous controls. SEPs from 75% of hypomorphic *ex117* homozygotes similarly lacked responses, while the other 25% of animals displayed only miniscule response blips

(Fig. 2C). Altogether, these data indicate a complete or almost complete lack of hearing function in both null and hypomorphic alleles. This deafness is attributable to *mir-279/996*, since the 16.6-kb *mir-279/996* genomic transgene rescued hearing function to levels indistinguishable from the controls (Fig. 2C,D).

miR-279/996 are functionally active in nonneural cells of the IO

To understand how miR-279/996 control JO organization, we needed to understand their spatial activity. To this end, we used a miR-279/996 sensor consisting of a ubiquitously transcribed *tub-GFP* sensor transgene bearing two antisense matches to miR-279 (Fig. 3A), which also served as miR-996 seed matches (Duan et al. 2018). This provided a negative readout of cells harboring functionally active miR-279/996 (which are GFP⁻).

The miRNA sensor was broadly silenced throughout JOs but was expressed in Elav* cells (Fig. 3B, top and middle rows), indicating that miR-279/996 activity is specifically low in neurons. To assess whether this spatial heterogeneity was truly due to miR-279/996, we analyzed the sensor in *mir-279/996[15C]* homozygotes. In this setting, the miR-279 sensor became broadly expressed across JOs (Fig. 3B, bottom row). We conclude that miR-279/996 are broadly active across the JO, except in JO neurons.

mir-279/996 autonomously prevent neural commitment by presumptive scolopale cells

Having examined the requirements of these miRNAs in whole-animal mutants, we analyzed their autonomous roles within the JO. Although directly nonautonomous roles for miRNAs are debated, there are reports of exosomal miRNAs in the nervous system (Fowler 2019) and some other settings. Systemic effects downstream from miRNA function are also plausible. For example, central peptidergic neurons control developmental timing and morphogenesis of peripheral organs (Yamanaka et al. 2013). We therefore made mitotic clones of *mir-279/996* [15C] and analyzed whether they disrupt JO lineages.

Although the JO is highly disorganized when the entire structure is mutant (Fig. 1), we can bypass this by generating small mutant clones in otherwise normal, heterozygous animals that are positively labeled using the MARCM system (Lee and Luo 1999). This allowed us to focus on autonomous defects with respect to cell fate. Since the neural (Elav⁺) and scolopale (Pros⁺) nuclei occupy adjacent rows within JOs, we could assess the identities of mutant (GFP+) cells within these cell layers (Fig. 3C). Control clones that overlap JOs, particularly within the layers that contain neuronal and scolopale cell nuclei, exhibit normal expression of Elav and Pros, respectively (Fig. 3D, top row). However, *mir-279/996[15C]* clones in this region fail to express Pros and exhibit ectopic Elay (Fig. 3D. middle rowl; occasionally, cells within the scolopale layer do not express either of these markers (Fig. 3D, bottom row). Quantification confirmed that miRNA mutant, Elav nuclei within the scolopale layer are the dominant

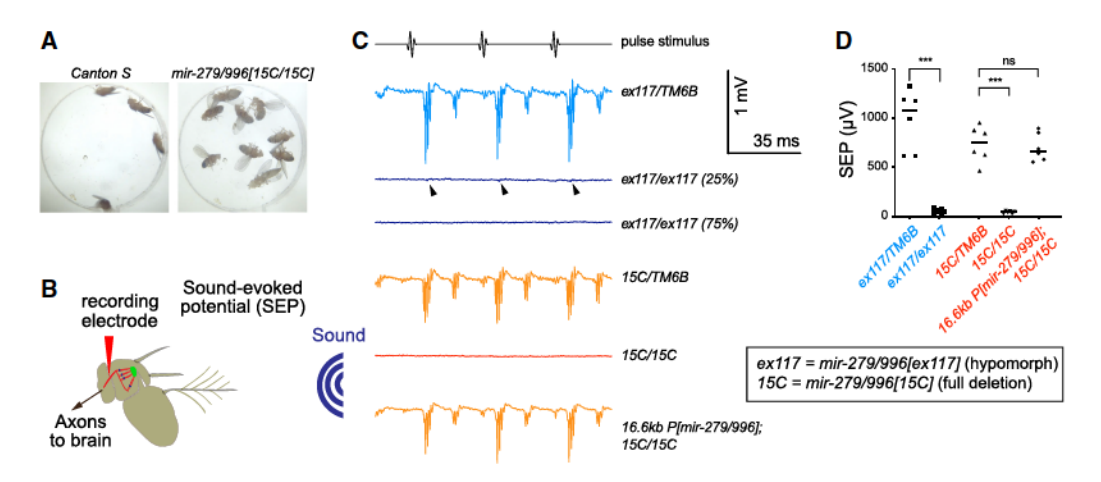


Figure 2. mir-279/996 are essential for locomotor coordination and hearing function. (A) Canton S wild-type flies (left) stand, groom, and walk, but mir-279/996[15C/15C]-null mutant flies (right) are completely uncoordinated and cannot perform any of these behaviors. (B) Schematic of auditory electrophysiology setup, showing JO sensory neurons in the A2 antennal segment (red) connected to the A3 segment stalk via dendritic caps (green). An electrode inserted into the joint between A1 and A2 recorded the extracellular activity (SEPs) of the antennal nerve containing JO neuron axons in response to near-field presentation of sound (blue). (C) Representative voltage traces (SEPs) recorded from the antennal nerve of the indicated genotypes in response to the computer-generated pulse stimulus. Compared with the large evoked spikes exhibited by heterozygous controls, homozygotes of the hypomorphic mir-279/996 allele ex117 are most often completely deaf (six out of eight antennae recorded), although two out of eight show tiny discernable blips (arrowheads) at the expected times after each stimulus pulse. Homozygotes of the null mir-279/996 allele 15C are completely deaf, and this is rescued by the 16.6-kb mir-279/996 genomic transgene. (D) Quantification of SEP recordings represented in C.

class (Fig. 3E). These data support the notion that these miRNAs autonomously prevent neural commitment by nonneural scolopale cells.

The Notch inhibitor insensible is limiting for mir-279/996 mutant defects in the IO lineage

In the mechanosensory bristle lineage, sheath cells in *mir*-279/996 mutants are selectively lost concomitant with ectopic neurons, a phenotype that is suggestive of compromised Notch signaling (Kavaler et al. 2018). For example, a full loss of Notch signaling during the bristle lineage causes all nonneuronal cells to adopt the neuronal fate (Hartenstein and Posakony 1990). Recently, we found that heterozygosity of *insensible* (*insb*), a direct miR-279/996 target that encodes a nuclear Notch inhibitor, is sufficient to nearly rescue sheath-to-neuron cell fate transformation in the mechanosensory bristle lineage of *mir-279/996* [15C] mutants (Kavaler et al. 2018).

The *insb*[Δ1] allele is a viable deletion encompassing four genes (Coumailleau and Schweisguth 2014). Accordingly, we used CRISPR/Cas9 to generate a targeted deletion of only the *insb* gene, replacing it with a 3xP3-DsRed marker (see Supplemental Fig. S4 for validation). The resulting *insb*[DsRed] allele was a definitive and specific null allele of *insb*, and the visible marker facilitated genetic manipulation. Like *insb*[Δ1], *insb*[DsRed] is also viable and appears developmentally normal. When introduced into 15C homozygotes, *insb*[DsRed]/+ conferred substantial rescue of JO development (Fig. 4A). However, while *insb* heterozygosity largely rescued *mir-279/996* [15C] mechanosensory organ lineage defects (Kavaler et al. 2018), we still observed a strong deficit of scolopale

cells in <code>insb[DsRed]/+;mir-279/996[15C]</code> JOs. This suggested that another miR-279/996 target might potentially contribute to the strong <code>mir-279/996</code> mutant JO phenotype.

Deregulation of two neuronal miR-279/996 targets is responsible for disruption of JO development and function

As is typical for miRNAs, there are >200 genes bearing well-conserved seed matches for miR-279/996 (e.g., see https://www.targetscan.org/fly_72). Indeed, many miR-279/996 targets were reported to be individually relevant across a variety of tissue settings (Cayirlioglu et al. 2008; Hartl et al. 2011; Yoon et al. 2011; Luo and Sehgal 2012; Laneve et al. 2013; Sun et al. 2015; Sanfilippo et al. 2016; Duan et al. 2018). However, if deregulation of several of these are causal for phenotype, it could be challenging to identify the appropriate set. It might be that no specific set of targets can explain a defect as profound as complete disruption of the JO, although negative results cannot be definitive.

The dissection and immunostaining of pupal JOs is delicate and demanding, and quantification of its cell types is laborious. Therefore, direct examination of JOs was not a favored strategy to evaluate many potential genetic modifiers. Instead, we took advantage of the fact that *mir-279/996*-null animals are extremely uncoordinated, which may reflect their overall proprioceptive deficit (Supplemental Fig. S5). Heterozygosity for either *insb[Δ1]* or *insb[DsRed]* substantially increased the capacity of *mir-279/996[15C]* mutants to stand, although they retained locomotor defects. We were especially curious to test miR-

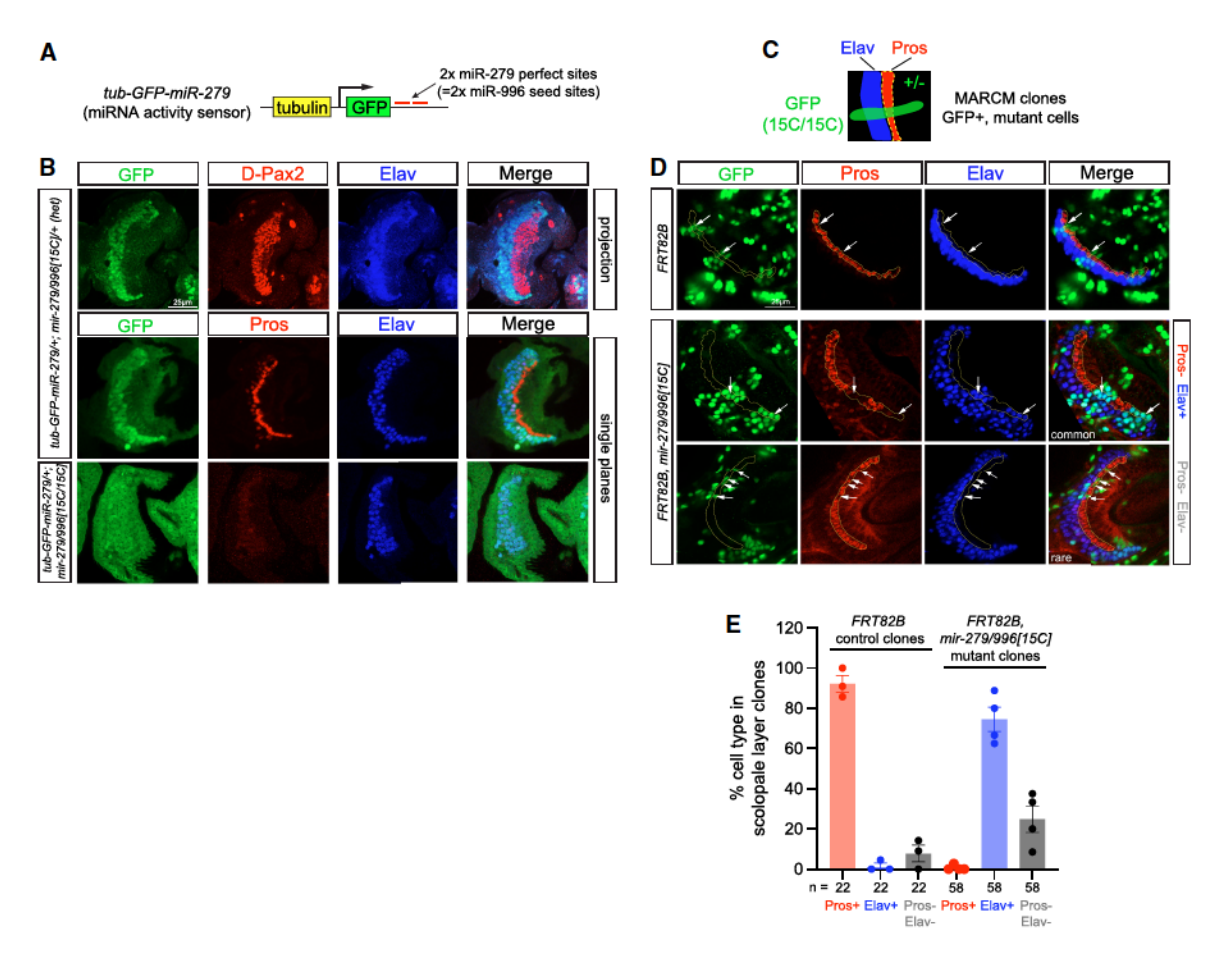


Figure 3. mir-279/996 act in nonneural cells of Johnston's organs to suppress neural fate. (A) miR-279/996 activity sensor. A ubiquitously transcribed tub-GFP-miR-279/996 reporter is repressed by both miR-279 (via perfect sites) and miR-996 (via seed matching). Thus, GFP staining is inversely correlated to miR-279/996 activity. Note that cytoplasmic GFP signals are displaced from the localization of nuclear cell fate markers, especially in single optical sections that are shown to emphasize the spatial heterogeneity of the sensor transgene. (B, top and middle) In control mir-279/996[15C] heterozygotes, the tub-GFP-miR-279/996 sensor is specifically elevated in Elav⁺ neurons. Other JO cells exhibit low GFP, including the layer of Pros⁺ scolopale cells adjacent to the neuronal layer. Both a projection and a single-plane image are shown for the control staining. The projection shows more JO cells but causes some cell stainings to overlap; the exclusion of high-sensor GFP from the Pros⁺ cell layer is emphasized in the single-plane image. (Bottom) The tub-GFP-miR-279/996 sensor shows relatively even spatial expression across mir-279/996[15C] JOs. (C) Schematic for MARCM analysis of homozygous mir-279/996[15C] clones that are positively marked by GFP. Because these clones are small, the overall organization of the JOs is preserved, unlike in whole-animal [15C] mutants (e.g., see Fig. 1C). (D, top) Control miRNA mutant clones that overlap the adjacent layers of neuronal and scolopale cell nuclei exhibit normal accumulation of Elav and Pros, respectively. (Middle) The major class of mir-279/996[15C] clones (n = 47 out of 58) that intersect the Pros⁺ layer exhibits loss of Pros and concomitant misexpression of Elav. (Bottom) A minor class of [15C] clones (n = 40 out of 58) lacks Pros but does not ectopically express Elav. (E) Quantification of cell types in control and mir-279/996[15C] clones within the scolopale layer, as marked by expression of Pros and Elav.

279/996 targets that had been related to sensory organ development, such as *nerfin* (Cayirlioglu et al. 2008), *ru* and *rho* (Duan et al. 2018), and *elav* (Sanfilippo et al. 2016). Although heterozygosity for *nerfin* and double heterozygosity for *ru* and *rho* had previously been reported to strongly rescue olfactory neuron defects and eye defects, respectively, these did not improve the ability of *mir-279/996[15C]* mutants to stand (Supplemental Fig. S5). Accordingly, these backgrounds did not rescue scolopale cell specification or differentiation (Supplemental Fig. S6). However, heterozygosity of the miR-279/996 target *elav*, which had not previously been associated with phenotypic impact on miRNA mutants, noticeably improved their ability to stand (Sup-

plemental Fig. S5). Nevertheless, JO development remained highly aberrant in these animals (Fig. 4A,B).

Excitingly, when we tested a double heterozygote of *elav + insb* in *mir-279/996[15C]* homozygotes, we observed strong rescue of both their ability to stand and their capacity to climb (Fig. 4D). In fact, these animals could walk normally, were capable of flight, and were even fertile. This encouraged us to conduct cytological analysis, which revealed nearly complete rescue of JO organization (Fig. 4A,B) and restoration of scolopale cells (Fig. 4C). Finally, we performed electrophysiological analysis of JO neurons during sound reception and also observed nearly full rescue of hearing in *elav;insb* double heterozygotes

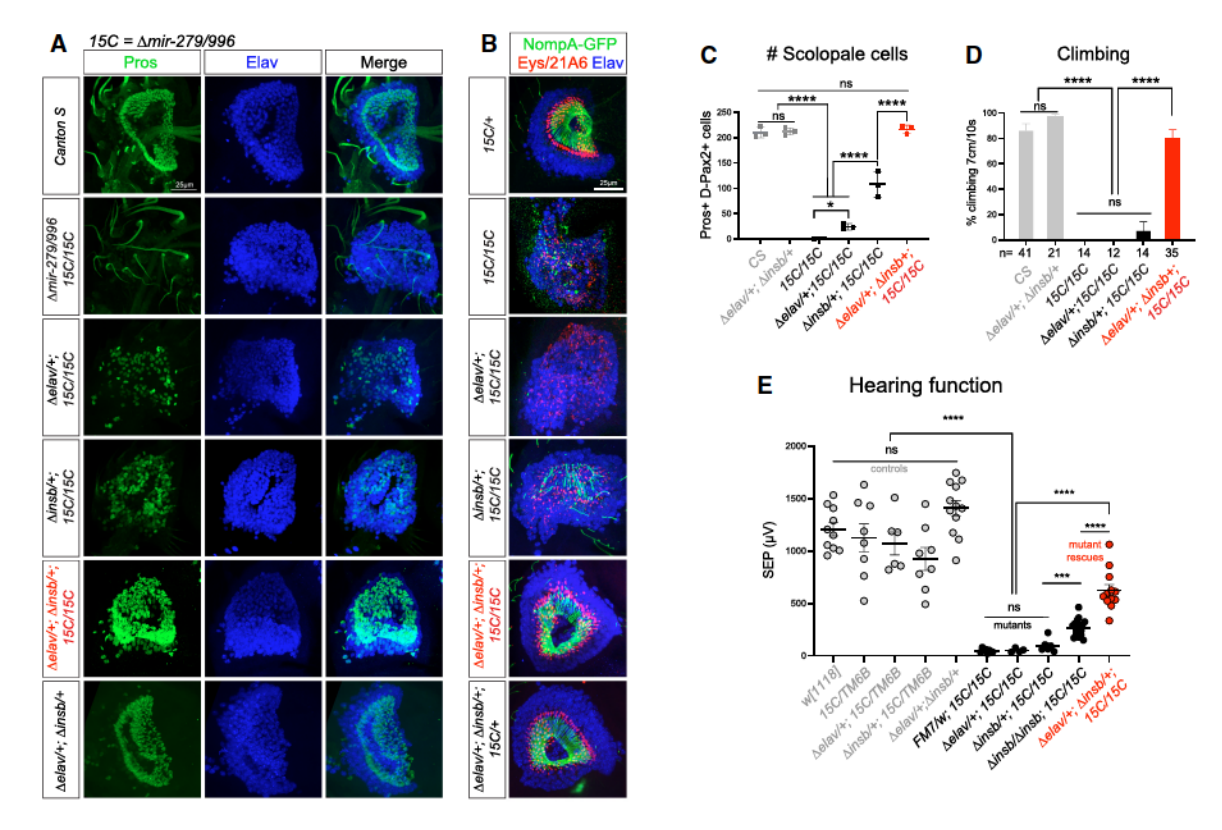


Figure 4. Neuronal *elav* and *insb* loci are critical targets for JO development and behavior. Dose-sensitive genetic interactions of miR-279/996 target mutants in *mir-279/996[15C]* homozygotes. (*A*, *B*) JO cytology. (*A*) JOs stained with Pros to label scolopale cells and with Elav to label neurons. *Canton S* and *15C* homozygotes exemplify normal and mutant JO development. *elav[CDS20]* heterozygotes exhibit only minor improvement of scolopale specification, whereas *insb[DsRed]* heterozygotes enable substantial development of Pros⁺ cells. Double heterozygotes of *elav[CDS20]* and *insb[DsRed]* exhibit nearly full rescue of JO cell specification. (*B*) JOs stained with markers that report on scolopale differentiation. NompA-GFP is expressed by scolopale cells, and Eys/21A6 is expressed by neurons but secreted into the scolopale space. This panel of genotypes exhibits JO phenotypes similar to those seen with nuclear markers (as shown in *A*), with double heterozygotes of *elav[CDS20]* and *insb[DsRed]* exhibiting nearly full rescue of scolopale cell differentiation. (*C*) Quantification of scolopale cells. Each dot represents quantification through the 3D volume of an individual Johnston's organ. (*D*) Quantification of negative geotaxis. (*E*) Quantification of hearing. All of these assays emphasize that double heterozygotes of *elav[CDS20]* and *insb[DsRed]* rescue *mir-279/996[15C]* homozygotes on a par with controls. (***) *P* < 0.001, (****) *P* < 0.0001, (ns) not significant; Student's *t*-test.

(Fig. 4E). Importantly, analysis of double-heterozygous *elav;insb* animals showed that they exhibit normal cytology, behavior, and electrophysiology (Fig. 4A–E). This confirmed that their profound suppression of miRNA deletion phenotypes is not a simple "cancelling" effect. Instead, the double-heterozygous background lacks substantial intrinsic defects but fully rescues one of the most overt miRNA knockout phenotypes known. Overall, misregulation of two direct miR-279/996 targets that are normally expressed in neuronal nuclei—the Notch corepressor Insb and the alternative mRNA processing factor Elav—underlies profound cell fate defects in *mir-279/996* mutant JOs that underlie deafness.

Discussion

Unlike the first recognized miRNAs (Lee et al. 1993; Reinhart et al. 2000), miRNA genes are generally dispensable for gross aspects of development, viability, or physiology (Miska et al. 2007; Alvarez-Saavedra and Horvitz

2010; Park et al. 2012; Chen et al. 2014) and have often been considered either to be used for fine-tuning of gene expression or to have selective impacts on stress conditions. In this study, we reveal a complete collapse of the *Drosophila* auditory system upon loss of a single miRNA locus, mir-279/996, and that this is attributable to specific discrete targets. Notch signaling is well appreciated to mediate cell fate specification throughout all tissues and organs and is famously highly dose-sensitive for normal development (Lai 2004). As such, it is perhaps logical that miRNA regulation of the Notch pathway might be required for appropriate cell choice (Lai 2002; Lai et al. 2005). Perhaps surprisingly, though, this is now the second developmental setting in which knockout of insb is normal, whereas its endogenous misexpression in a miRNA knockout is highly deleterious (Kavaler et al. 2018). This highlights the fact that normal developmental programs are not necessarily optimally designed but may instead be the result of genetic histories and happenstance that are not fully relevant in present-day animals.

The regulatory rationale is less clear for Elay, which is classically considered to be a neural marker; i.e., a gene whose function is exerted after the decision to become a postmitotic neuron (Wei and Lai 2022). However, in reality, elav is detectably transcribed and translated ubiquitously albeit modestly (Sanfilippo et al. 2016), and its broader nonneural expression is increasingly appreciated via scRNA profiling (Seroka et al. 2022), including within neural progenitors and glial cells (Berger et al. 2007; Lai et al. 2012; Konstantinides et al. 2022). Elav was long inferred to be a post-transcriptional regulator, owing to its RNA binding domains. However, only recently were its myriad roles in alternative splicing and alternative polyadenylation established (Carrasco et al. 2020; Wei et al. 2020; Lee et al. 2021). We show here that elav exhibits dominant genetic interactions that suppress ectopic neural fate in mir-279/996 mutants, particularly evident when insb is heterozygous. To our knowledge, this is the first overt role described for Elav to promote neural cell fate choice. This may conceivably relate to the broad, latent capacity for neurogenesis throughout epithelial tissues (Lehmann et al. 1983), coupled to the suppression of ubiquitously transcribed *elav* by miR-279/996 (Sanfilippo et al. 2016).

In summary, the development and function of chordotonal organs that comprise the *Drosophila* auditory system relies on miRNA control of both transcriptional and post-transcriptional neural regulators.

Materials and methods

Drosophila stocks

Drosophila mutants and transgenes used in this study included mir-279/996[15C], mir-279/996[ex117], and P[16.6kb mir-279/996] (Sun et al. 2015); Df(3R)Exel6212/TM6B, which deletes mir-279/996 (Bloomington 7690); tub-GFP-2x-miR-279 (Duan et al. 2018); FRT82B, mir-279/996[15C] (Kavaler et al. 2018); hsFLP, UAS-GFP;tub-Gal4;FRT82B tub-Gal80/TM6B (Sanfilippo et al. 2016); NompA-GFP (gift of Maurice Kernan, State University of New York, Stony Brook) (Chung et al. 2001), insb[\Delta1] (gift of Francois Schweisguth, Institut Pasteur) (Coumailleau and Schweisguth 2014); elav[5] (gift of M. Soller, University of Birmingham) (Yao et al. 1993); and elav[CDS20] (gift of Valerie Hilgers, Max Planck Institute, Freiburg) (Carrasco et al. 2020).

CRISPR/Cas9-mediated deletion of insb

We used the pHD-attP-DsRed donor vector (Gratz et al. 2014) carrying ~1-kb homology arms that were amplified from genomic DNA. The donor arms were adjacent to pairs of gRNAs that target upstream of and downstream from the *insb* transcription unit (detailed in Supplemental Fig. S4). The four gRNAs were cloned into pCFD5, which allowed multiple tRNA-flanked gRNAs to be coexpressed and excised (Port and Bullock 2016). The plasmids were coinjected by BestGene, and DsRed+ candidate progeny were identified. We verified on-target insertion of DsRed and concomitant deletion of *insb* using PCR. Primers for donor arm amplification, gRNA inserts, and *insb[DsRed]* genotyping are listed in Supplemental Table S1.

Drosophila immunostaining

Staged pupae were obtained by collecting them at the white prepupal stage and then aging them 45 h before antennal dissection in cold PBS using Dumont #5 forceps (Fine Science Tools). Antennae were fixed in 4% paraformaldehyde in PBS (Sigma Aldrich) for 1 h at room temperature, followed by two 30-min washes in PBS with 0.2% Tween 20 (PBST). The following primary antibodies were used: rabbit anti-D-Pax2 (1:10,000) (Kavaler et al. 2018), mouse anti-Futsch/22C10 (1:500; Developmental Studies Hybridoma Bank [DSHB]), rat anti-Elav (1:200; DSHB), mouse anti-Elav (1:100; DSHB), mouse anti-Pros (1:100; DSHB), and mouse anti-Eys/21A6 (1:100; DSHB). Samples were incubated with the primary antibody for 1 d at 4°C with gentle rotation, followed by two 30-min washes in PBST. Secondary antibodies were goat antirabbit IgG Alexa fluor 555, goat antimouse IgG Alexa fluor 488, and goat antirat lgG Alexa fluor 633 (each 1:1000; Invitrogen). Samples were incubated in secondary antibodies for 1 d at 4°C with gentle rotation, followed by two 30-min washes in PBST. Samples were incubated with DAPI in PBS for 1 h at room temperature before mounting. Imaging was performed on a Leica SP5 confocal microscope using HCX PL APO 63×/~0.70 and HCX PL APO 100×/~1.25-0.75 lenses and processed using Fiji.

Clonal analysis in the Johnston's organ

Positively marked mitotic clones were produced using the MARCM technique (Lee and Luo 1999). Control clones used were as follows: *y, w, hs-FLP, UAS-nlsGFP/+* or *Y;FRT82/tub-gal4, FRT82B, tub-gal80. mir-279/996* deletion clones used were as follows: *y, w, hs-FLP, UAS-nlsGFP/+* or *Y;FRT82, mir-279/996[15C]/tub-gal4, FRT82B, tub-gal80.* Larvae at L2–L3 stages were heat-shocked for 60 min at 37°C and then reared at 25°C until 45 h APF before dissection.

Electrophysiological recordings

Sound-evoked potential (SEP) recordings were performed from the antennal nerve as described (Eberl and Kernan 2011). Briefly, using a custom LabView (National Instruments) virtual instrument, computer-generated pulse song was delivered frontally from a loudspeaker in the near field to the fly's head through Tygon tubing. Electrolytically sharpened tungsten electrodes were inserted-one dorso-medially between the first and second antennal segments, and the second as a reference electrode penetrating the dorsal head cuticle. Differential signals were amplified 1000×, filtered with a 10-Hz low filter to stabilize the baseline, digitized with a USB-6001 (National Instruments) data acquisition module, and recorded in the LabView virtual instrument. Amplitudes are measured from the average of 10 consecutive recordings from each antenna. Flies of different genotypes were recorded in alternate order to minimize systematic variations. Statistical analysis used pairwise t-tests, with Welch's correction applied when variances were unequal.

Competing interest statement

The authors declare no competing interests.

Acknowledgments

We thank Bidisha Roy for preliminary cytological studies, Samantha Fleishman for preliminary behavioral analyses, and Lijuan Kan for helpful discussions. We acknowledge Maurice Kernan, François Schweisguth, Matthias Soller, and Valerie Hilgers for *Drosophila* stocks used in this study. We thank the Developmental Studies Hybridoma Bank (DSHB) for providing high-quality, cost-effective, monoclonal antibodies, and the Bloomington Stock Center for reliable provision of fly stocks. Work in D.F.E.'s group was supported by the National Science Foundation (NSF 2037828). Work in E.C.L.'s group was supported by the National Institutes of Health (R01-NS083833 and R01-GM083300) and Memorial Sloan Kettering Core grant P30-CA008748.

Author contributions: B.Z., H.D., and J.K. performed genetic and cytological studies. L.W. performed CRISPR/Cas9 mutagenesis. D.F.E. performed electrophysiological studies. E.C.L. oversaw the project, obtained funding, and wrote the manuscript with input from all of the authors.

References

- Agarwal V, Bell GW, Nam JW, Bartel DP. 2015. Predicting effective microRNA target sites in mammalian mRNAs. Elife 4: e05005. doi:10.7554/eLife.05005
- Albert JT, Nadrowski B, Göpfert MC. 2007. Mechanical signatures of transducer gating in the *Drosophila* ear. *Curr Biol* 17: 1000–1006. doi:10.1016/j.cub.2007.05.004
- Albert JT, Jarman AP, Kamikouchi A, Keder A. 2020. Drosophila as a model for hearing and deafness. In The senses: a comprehensive reference (ed. Fritzsch B), pp. 985–1004. Elsevier Academic Press, Cambridge, MA.
- Alvarez-Saavedra E, Horvitz HR. 2010. Many families of C. elegans microRNAs are not essential for development or viability. Curr Biol 20: 367–373. doi:10.1016/j.cub.2009.12.051
- Armstrong JD, Texada MJ, Munjaal R, Baker DA, Beckingham KM. 2006. Gravitaxis in *Drosophila melanogaster*: a forward genetic screen. *Genes Brain Behav* 5: 222–239. doi:10.1111/j.1601-183X.2005.00154.x
- Avetisyan A, Glatt Y, Cohen M, Timerman Y, Aspis N, Nachman A, Halachmi N, Preger-Ben Noon E, Salzberg A. 2021. Delilah, prospero, and D-Pax2 constitute a gene regulatory network essential for the development of functional proprioceptors. *Elife* 10: e70833. doi:10.7554/eLife.70833
- Avraham KB, Khalaily L, Noy Y, Kamal L, Koffler-Brill T, Taiber S. 2022. The noncoding genome and hearing loss. *Hum Genet* 141: 323–333. doi:10.1007/s00439-021-02359-z
- Berger C, Renner S, Lüer K, Technau GM. 2007. The commonly used marker ELAV is transiently expressed in neuroblasts and glial cells in the *Drosophila* embryonic CNS. *Dev Dyn* 236: 3562–3568. doi:10.1002/dvdy.21372
- Bermingham NA, Hassan BA, Price SD, Vollrath MA, Ben-Arie N, Eatock RA, Bellen HJ, Lysakowski A, Zoghbi HY. 1999. Math 1: an essential gene for the generation of inner ear hair cells. Science 284: 1837–1841. doi:10.1126/science.284.5421 .1837
- Boekhoff-Falk G, Eberl DF. 2014. The *Drosophila* auditory system. *Wiley Interdiscip Rev Dev Biol* 3: 179–191. doi:10 .1002/wdev.128
- Boo KS, Richards AG. 1975. Fine structure of scolopidia in Johnston's organ of female aedes aegypti compared with that of the male. *J Insect Physiol* 21: 1129–1139. doi:10.1016/0022-1910 (75)90126-2
- Cachero S, Simpson TI, Zur Lage PI, Ma L, Newton FG, Holohan EE, Armstrong JD, Jarman AP. 2011. The gene regulatory cascade linking proneural specification with differentiation in *Drosophila* sensory neurons. *PLoS Biol* 9: e1000568. doi:10.1371/journal.pbio.1000568

- Caldwell JC, Eberl DF. 2002. Towards a molecular understanding of *Drosophila* hearing. J Neurobiol 53: 172–189. doi:10.1002/ neu.10126
- Carrasco J, Rauer M, Hummel B, Grzejda D, Alfonso-Gonzalez C, Lee Y, Wang Q, Puchalska M, Mittler G, Hilgers V. 2020. ELAV and FNE determine neuronal transcript signatures through EXon-activated rescue. *Mol Cell* 80: 156–163.e6. doi:10.1016/j.molcel.2020.09.011
- Cayirlioglu P, Kadow IG, Zhan X, Okamura K, Suh GS, Gunning D, Lai EC, Zipursky SL. 2008. Hybrid neurons in a microRNA mutant are putative evolutionary intermediates in insect CO₂ sensory systems. *Science* 319: 1256–1260. doi:10.1126/science.1149483
- Chen YW, Song S, Weng R, Verma P, Kugler JM, Buescher M, Rouam S, Cohen SM. 2014. Systematic study of *Drosophila* microRNA functions using a collection of targeted knockout mutations. *Dev Cell* 31: 784–800. doi:10.1016/j.devcel.2014 .11.029
- Christie KW, Eberl DF. 2014. Noise-induced hearing loss: new animal models. *Curr Opin Otolaryngol Head Neck Surg* 22: 374–383. doi:10.1097/MOO.0000000000000086
- Chung YD, Zhu J, Han Y, Kernan MJ. 2001. Nompa encodes a PNS-specific, ZP domain protein required to connect mechanosensory dendrites to sensory structures. *Neuron* 29: 415– 428. doi:10.1016/S0896-6273(01)00215-X
- Coumailleau F, Schweisguth F. 2014. Insensible is a novel nuclear inhibitor of notch activity in *Drosophila*. *PLoS ONE* 9: e98213. doi:10.1371/journal.pone.0098213
- Dror AA, Avraham KB. 2009. Hearing loss: mechanisms revealed by genetics and cell biology. *Ann Rev Genetics* 43: 411–437. doi:10.1146/annurev-genet-102108-134135
- Duan H, de Navas LF, Hu F, Sun K, Mavromatakis YE, Viets K, Zhou C, Kavaler J, Johnston RJ, Tomlinson A, et al. 2018. The mir-279/996 cluster represses receptor tyrosine kinase signaling to determine cell fates in the Drosophila eye. Development 145: dev159053. doi:10.1242/dev.159053
- Eberl DF, Boekhoff-Falk G. 2007. Development of Johnston's organ in *Drosophila*. *Int J Dev Biol* 51: 679–687. doi:10.1387/ijdb.072364de
- Eberl DF, Kernan MJ. 2011. Recording sound-evoked potentials from the *Drosophila* antennal nerve. *Cold Spring Harb Protoc* 2011: prot5576. doi:10.1101/pdb.prot5576
- Eberl DF, Hardy RW, Kernan MJ. 2000. Genetically similar transduction mechanisms for touch and hearing in *Drosophila*. J Neurosci 20: 5981–5988. doi:10.1523/JNEUROSCI.20-16-05981.2000
- Fowler CD. 2019. NeuroEVs: characterizing extracellular vesicles generated in the neural domain. *J Neurosci* **39**: 9262–9268. doi:10.1523/JNEUROSCI.0146-18.2019
- Fritzsch B, Erives A, Eberl DF, Yamoah EN. 2020. Genetics of mechanoreceptor evolution and development. In *The senses:* a comprehensive reference (ed. Fritzsch B), pp. 277–301. Elsevier Academic Press, Cambridge, MA.
- Gratz SJ, Ukken FP, Rubinstein CD, Thiede G, Donohue LK, Cummings AM, O'Connor-Giles KM. 2014. Highly specific and efficient CRISPR/Cas9-catalyzed homology-directed repair in *Drosophila*. *Genetics* 196: 961–971. doi:10.1534/genet ics.113.160713
- Hartenstein V, Posakony JW. 1990. A dual function of the *Notch* gene in *Drosophila* sensillum development. *Dev Biol* 142: 13–30. doi:10.1016/0012-1606(90)90147-B
- Hartl M, Loschek LF, Stephan D, Siju KP, Knappmeyer C, Kadow IC. 2011. A new Prospero and microRNA-279 pathway restricts CO₂ receptor neuron formation. J Neurosci 31: 15660–15673. doi:10.1523/INEUROSCI.2592-11.2011

- Hildebrand MS, Newton SS, Gubbels SP, Sheffield AM, Kochhar A, de Silva MG, Dahl HM, Rose SD, Behlke MA, Smith RJ. 2008. Advances in molecular and cellular therapies for hearing loss. *Mol Ther* 16: 224–236. doi:10.1038/sj.mt.6300351
- Ishikawa Y, Fujiwara M, Wong J, Ura A, Kamikouchi A. 2019. Stereotyped combination of hearing and wind/gravity-sensing neurons in the Johnston's organ of *Drosophila*. Front Physiol 10: 1552. doi:10.3389/fphys.2019.01552
- Jarman AP. 2014. Development of the auditory organ (Johnston's organ) in *Drosophila*. In *Development of auditory and vestibular systems* (ed. Romand R, Varela-Nieto I), pp. 31–61. Academic Press, San Diego.
- Jarman AP, Groves AK. 2013. The role of atonal transcription factors in the development of mechanosensitive cells. Semin Cell Dev Bio 24: 438–447. doi:10.1016/j.semcdb.2013.03.010
- Jarman AP, Grau Y, Jan LY, Jan YN. 1993. Atonal is a proneural gene that directs chordotonal organ formation in the Drosophila peripheral nervous system. Cell 73: 1307–1321. doi:10 .1016/0092-8674(93)90358-W
- Kamikouchi A, Shimada T, Ito K. 2006. Comprehensive classification of the auditory sensory projections in the brain of the fruit fly *Drosophila melanogaster*. J Comp Neuro 499: 317– 356. doi:10.1002/cne.21075
- Kamikouchi A, Inagaki HK, Effertz T, Hendrich O, Fiala A, Göpfert MC, Ito K. 2009. The neural basis of *Drosophila* gravity-sensing and hearing. *Nature* 458: 165–171. doi:10.1038/nature07810
- Kavaler J, Duan H, Aradhya R, de Navas LF, Joseph B, Shklyar B, Lai EC. 2018. miRNA suppression of a Notch repressor directs non-neuronal fate in *Drosophila* mechanosensory organs. J Cell Biol 217: 571–583. doi:10.1083/jcb.201706101
- Kavlie RG, Albert JT. 2013. Transduction and amplification in the ear: insights from insects. In *Insights from comparative* hearing research (ed. Köppl C, et al.), pp. 13–35. Springer, New York.
- Konstantinides N, Holguera I, Rossi AM, Escobar A, Dudragne L, Chen YC, Tran TN, Martínez Jaimes AM, Özel MN, Simon F, et al. 2022. A complete temporal transcription factor series in the fly visual system. *Nature* 604: 316–322. doi:10.1038/ s41586-022-04564-w
- Kuhn S, Johnson SL, Furness DN, Chen J, Ingham N, Hilton JM, Steffes G, Lewis MA, Zampini V, Hackney CM, et al. 2011. miR-96 regulates the progression of differentiation in mammalian cochlear inner and outer hair cells. *Proc Natl Acad Sci* 108: 2355–2360. doi:10.1073/pnas.1016646108
- Lai EC. 2002. MicroRNAs are complementary to 3' UTR sequence motifs that mediate negative post-transcriptional regulation. Nat Genet 30: 363–364. doi:10.1038/ng865
- Lai EC. 2004. Notch signaling: control of cell communication and cell fate. Development 131: 965–973. doi:10.1242/dev.01074
- Lai EC, Orgogozo V. 2004. A hidden program in *Drosophila* peripheral neurogenesis revealed: fundamental principles underlying sensory organ diversity. *Dev Biol* 269: 1–17. doi:10.1016/j.ydbio.2004.01.032
- Lai EC, Tam B, Rubin GM. 2005. Pervasive regulation of *Drosophila* Notch target genes by GY-box-, Brd-box-, and K-box-class microRNAs. *Genes Dev* 19: 1067–1080. doi:10.1101/gad.1291905
- Lai SL, Miller MR, Robinson KJ, Doe CQ. 2012. The Snail family member Worniu is continuously required in neuroblasts to prevent Elav-induced premature differentiation. *Dev Cell* 23: 849–857. doi:10.1016/j.devcel.2012.09.007
- Laneve P, Delaporte C, Trebuchet G, Komonyi O, Flici H, Popkova A, D'Agostino G, Taglini F, Kerekes I, Giangrande A. 2013. The Gcm/Glide molecular and cellular pathway: new

- actors and new lineages. Dev Biol 375: 65-78. doi:10.1016/j .ydbio.2012.12.014
- Lee T, Luo L. 1999. Mosaic analysis with a repressible cell marker for studies of gene function in neuronal morphogenesis. *Neu*ron 22: 451–461. doi:10.1016/S0896-6273(00)80701-1
- Lee RC, Feinbaum RL, Ambros V. 1993. The C. elegans heterochronic gene lin-4 encodes small RNAs with antisense complementarity to lin-14. Cell 75: 843–854. doi:10.1016/0092-8674(93)90529-Y
- Lee S, Wei L, Zhang B, Goering R, Majumdar S, Wen J, Taliaferro JM, Lai EC. 2021. ELAV/hu RNA binding proteins determine multiple programs of neural alternative splicing. *PLoS Genet* 17: e1009439. doi:10.1371/journal.pgen.1009439
- Lehmann R, Jiménez F, Dietrich U, Campos-Ortega J. 1983. On the phenotype and development of mutants of early neurogenesis in *Drosophila melanogaster*. Roux's Arch Dev Biol 192: 62–74. doi:10.1007/BF00848482
- Lewis MA, Quint E, Glazier AM, Fuchs H, De Angelis MH, Langford C, van Dongen S, Abreu-Goodger C, Piipari M, Redshaw N, et al. 2009. An ENU-induced mutation of miR-96 associated with progressive hearing loss in mice. Nat Genet 41: 614–618. doi:10.1038/ng.369
- Lewis MA, Di Domenico F, Ingham NJ, Prosser HM, Steel KP. 2020. Hearing impairment due to mir183/96/182 mutations suggests both loss and gain of function effects. Dis Model Mech 41: dmm047225. doi:10.1242/dmm.047225
- Li T, Bellen HJ, Groves AK. 2018. Using *Drosophila* to study mechanisms of hereditary hearing loss. *Dis Model Mech* 11: dmm031492. doi:10.1242/dmm.031492
- Li XJ, Morgan C, Goff LA, Doetzlhofer A. 2022. Follistatin promotes LIN28B-mediated supporting cell reprogramming and hair cell regeneration in the murine cochlea. Sci Adv 8: eabj7651. doi:10.1126/sciadv.abj7651
- Lin FR, Niparko JK, Ferrucci L. 2011. Hearing loss prevalence in the United States. Arch Intern Med 171: 1851–1852. doi:10 .1001/archinternmed.2011.506
- Lu Q, Senthilan PR, Effertz T, Nadrowski B, Gopfert MC. 2009. Using *Drosophila* for studying fundamental processes in hearing. *Integr Comp Biol* 49: 674–680. doi:10.1093/icb/icp072
- Luo W, Sehgal A. 2012. Regulation of circadian behavioral output via a microRNA–JAK/STAT circuit. Cell 148: 765–779. doi:10 .1016/j.cell.2011.12.024
- Lynch ED, Lee MK, Morrow JE, Welcsh PL, León PE, King MC. 1997. Nonsyndromic deafness DFNA1 associated with mutation of a human homolog of the *Drosophila* gene *diaphanous*. *Science* 278: 1315–1318. doi:10.1126/science.278.5341.1315
- Mahato S, Nie J, Plachetzki DC, Zelhof AC. 2018. A mosaic of independent innovations involving eyes shut are critical for the evolutionary transition from fused to open rhabdoms. *Dev Biol* 443: 188–202. doi:10.1016/j.ydbio.2018.09.016
- Miska EA, Alvarez-Saavedra E, Abbott AL, Lau NC, Hellman AB, McGonagle SM, Bartel DP, Ambros VR, Horvitz HR. 2007. Most Caenorhabditis elegans microRNAs are individually not essential for development or viability. PLoS Genet 3: e215. doi:10.1371/journal.pgen.0030215
- Nakano Y, Wiechert S, Fritzsch B, Bánfi B. 2020. Inhibition of a transcriptional repressor rescues hearing in a splicing factordeficient mouse. *Life Sci Alliance* 3: e202000841. doi:10 .26508/lsa.202000841
- Nolan LS, Chen J, Gonçalves AC, Bullen A, Towers ER, Steel KP, Dawson SJ, Gale JE. 2022. Targeted deletion of the RNA-binding protein Caprin1 leads to progressive hearing loss and impairs recovery from noise exposure in mice. Sci Reports 12: 2444. doi:10.1038/s41598-022-05657-2

- Park CY, Jeker LT, Carver-Moore K, Oh A, Liu HJ, Cameron R, Richards H, Li Z, Adler D, Yoshinaga Y, et al. 2012. A resource for the conditional ablation of microRNAs in the mouse. *Cell Rep* 1: 385–391. doi:10.1016/j.celrep.2012.02.008
- Petit C. 2006. From deafness genes to hearing mechanisms: harmony and counterpoint. *Trends Mol Med* 12: 57–64. doi:10 .1016/j.molmed.2005.12.006
- Pierce ML, Weston MD, Fritzsch B, Gabel HW, Ruvkun G, Soukup GA. 2008. MicroRNA-183 family conservation and ciliated neurosensory organ expression. Evol Dev 10: 106– 113. doi:10.1111/j.1525-142X.2007.00217.x
- Port F, Bullock SL. 2016. Augmenting CRISPR applications in Drosophila with tRNA-flanked sgRNAs. Nat Methods 13: 852–854. doi:10.1038/nmeth.3972
- Ray D, Kazan H, Cook KB, Weirauch MT, Najafabadi HS, Li X, Gueroussov S, Albu M, Zheng H, Yang A, et al. 2013. A compendium of RNA-binding motifs for decoding gene regulation. Nature 499: 172–177. doi:10.1038/nature12311
- Reinhart BJ, Slack F, Basson M, Pasquinelli A, Bettinger J, Rougvie A, Horvitz HR, Ruvkun G. 2000. The 21-nucleotide *let-7* RNA regulates developmental timing in *Caenorhabditis elegans*. *Nature* 403: 901–906. doi:10.1038/35002607
- Sanfilippo P, Smibert P, Duan H, Lai EC. 2016. Neural specificity of the RNA-binding protein elav is achieved by post-transcriptional repression in non-neural tissues. *Development* 143: 4474–4485. doi:10.1242/dev.141978
- Schoen CJ, Emery SB, Thorne MC, Ammana HR, Śliwerska E, Arnett J, Hortsch M, Hannan F, Burmeister M, Lesperance MM. 2010. Increased activity of *Diaphanous homolog 3* (*DIAPH3*)/diaphanous causes hearing defects in humans with auditory neuropathy and in *Drosophila*. Proc Natl Acad Sci 107: 13396–13401. doi:10.1073/pnas.1003027107
- Seroka A, Lai SL, Doe CQ. 2022. Transcriptional profiling from whole embryos to single neuroblast lineages in *Drosophila*. *Dev Biol* 489: 21–33. doi:10.1016/j.ydbio.2022.05.018
- Shi DL, Cheng XN, Saquet A, Grifone R. 2022. Emerging roles of RNA-binding proteins in inner ear hair cell development and regeneration. *Int J Mol Sci* 23: 12393. doi:10.3390/ ijms232012393
- Singh SP, Mohan L. 2013. Variations in the ommatidia and compound eye of three species of mosquito vectors. *J Entomol Zool Stud* 1: 16–21.
- Sun K, Jee D, de Navas LF, Duan H, Lai EC. 2015. Multiple in vivo biological processes are mediated by functionally redundant activities of *Drosophila mir-279* and *mir-996*. *PLoS Genet* 11: e1005245. doi:10.1371/journal.pgen.1005245

- Todi SV, Sharma Y, Eberl DF. 2004. Anatomical and molecular design of the *Drosophila* antenna as a flagellar auditory organ. *Microsc Res Tech* 63: 388–399. doi:10.1002/jemt.20053
- Todi SV, Franke JD, Kiehart DP, Eberl DF. 2005. Myosin VIIA defects, which underlie the usher 1B syndrome in humans, lead to deafness in *Drosophila*. *Curr Biol* 15: 862–868. doi:10.1016/j.cub.2005.03.050
- Todi SV, Sivan-Loukianova E, Jacobs JS, Kiehart DP, Eberl DF. 2008. Myosin VIIA, important for human auditory function, is necessary for *Drosophila* auditory organ development. *PLoS ONE* 3: e2115. doi:10.1371/journal.pone.0002115
- Van Nostrand EL, Freese P, Pratt GA, Wang X, Wei X, Xiao R, Blue SM, Chen JY, Cody NAL, Dominguez D, et al. 2020. A large-scale binding and functional map of human RNA-binding proteins. *Nature* 583: 711–719. doi:10.1038/s41586-020-2077-3
- Wei L, Lai EC. 2022. Regulation of the alternative neural transcriptome by ELAV/Hu RNA binding proteins. Front Genet 13: 848626. doi:10.3389/fgene.2022.848626
- Wei L, Lee S, Majumdar S, Zhang B, Sanfilippo P, Joseph B, Miura P, Soller M, Lai EC. 2020. Overlapping activities of ELAV/Hu family RNA binding proteins specify the extended neuronal 3′ UTR landscape in *Drosophila*. *Mol Cell* 80: 140–155.e6. doi:10 .1016/j.molcel.2020.09.007
- Yamanaka N, Rewitz KF, O'Connor MB. 2013. Ecdysone control of developmental transitions: lessons from *Drosophila* research. *Annu Rev Entomol* 58: 497–516. doi:10.1146/ annurev-ento-120811-153608
- Yao KM, Samson ML, Reeves R, White K. 1993. Gene elav of Drosophila melanogaster: a prototype for neuronal-specific RNA binding protein gene family that is conserved in flies and humans. J Neurobiol 24: 723–739. doi:10.1002/neu.480240604
- Yoon WH, Meinhardt H, Montell DJ. 2011. miRNA-mediated feedback inhibition of JAK/STAT morphogen signalling establishes a cell fate threshold. Nat Cell Biol 13: 1062–1069. doi:10 .1038/ncb2316
- Yorozu S, Wong A, Fischer BJ, Dankert H, Kernan MJ, Kamikouchi A, Ito K, Anderson DJ. 2009. Distinct sensory representations of wind and near-field sound in the *Drosophila* brain. *Nature* 458: 201–205. doi:10.1038/nature07843
- Zine A, Aubert A, Qiu J, Therianos S, Guillemot F, Kageyama R, de Ribaupierre F. 2001. Hes1 and Hes5 activities are required for the normal development of the hair cells in the mammalian inner ear. J Neurosci 21: 4712–4720. doi:10.1523/JNEURO SCI.21-13-04712.2001



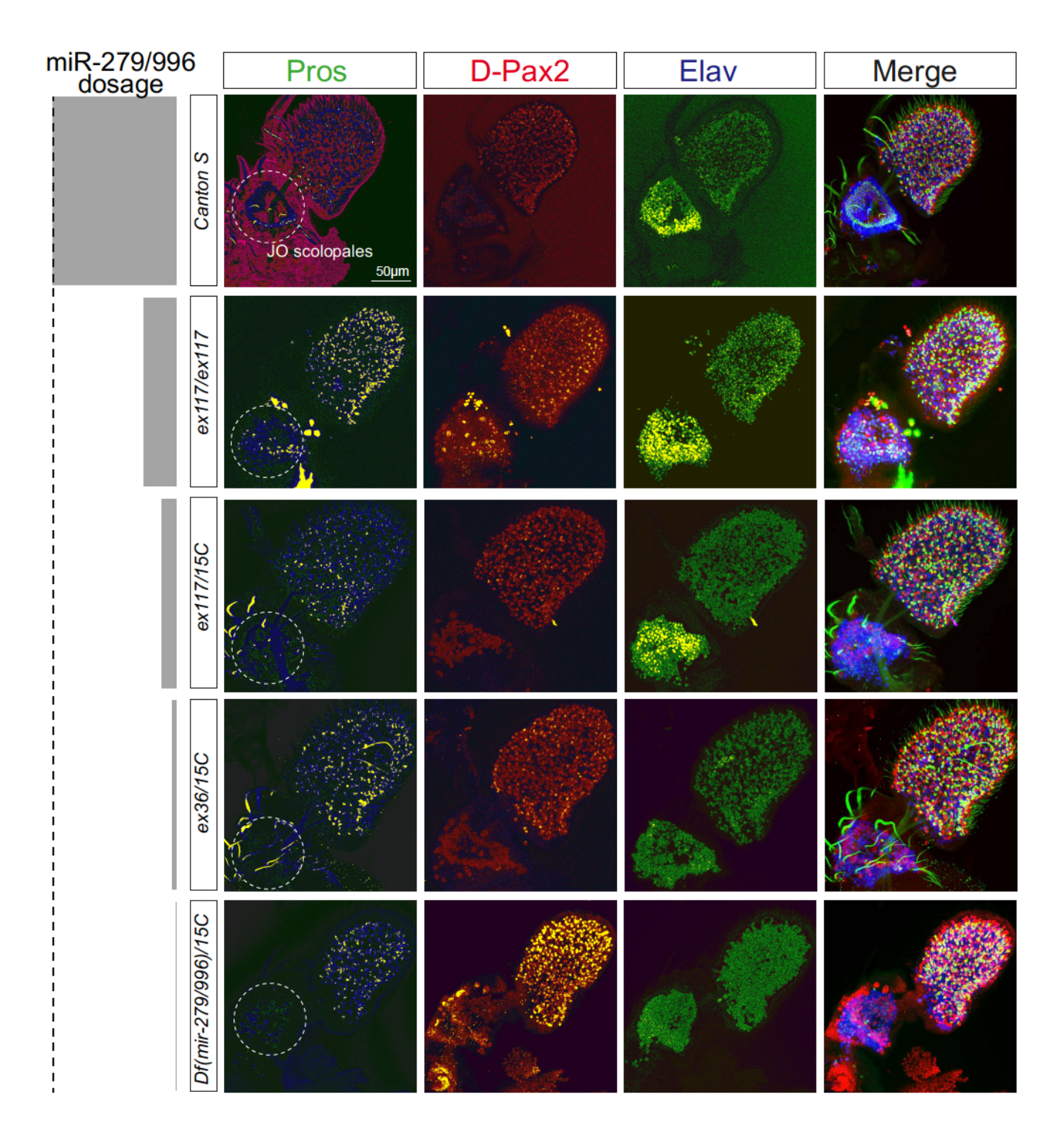
A nonneural miRNA cluster mediates hearing via repression of two neural targets

Binglong Zhang, Hong Duan, Joshua Kavaler, et al.

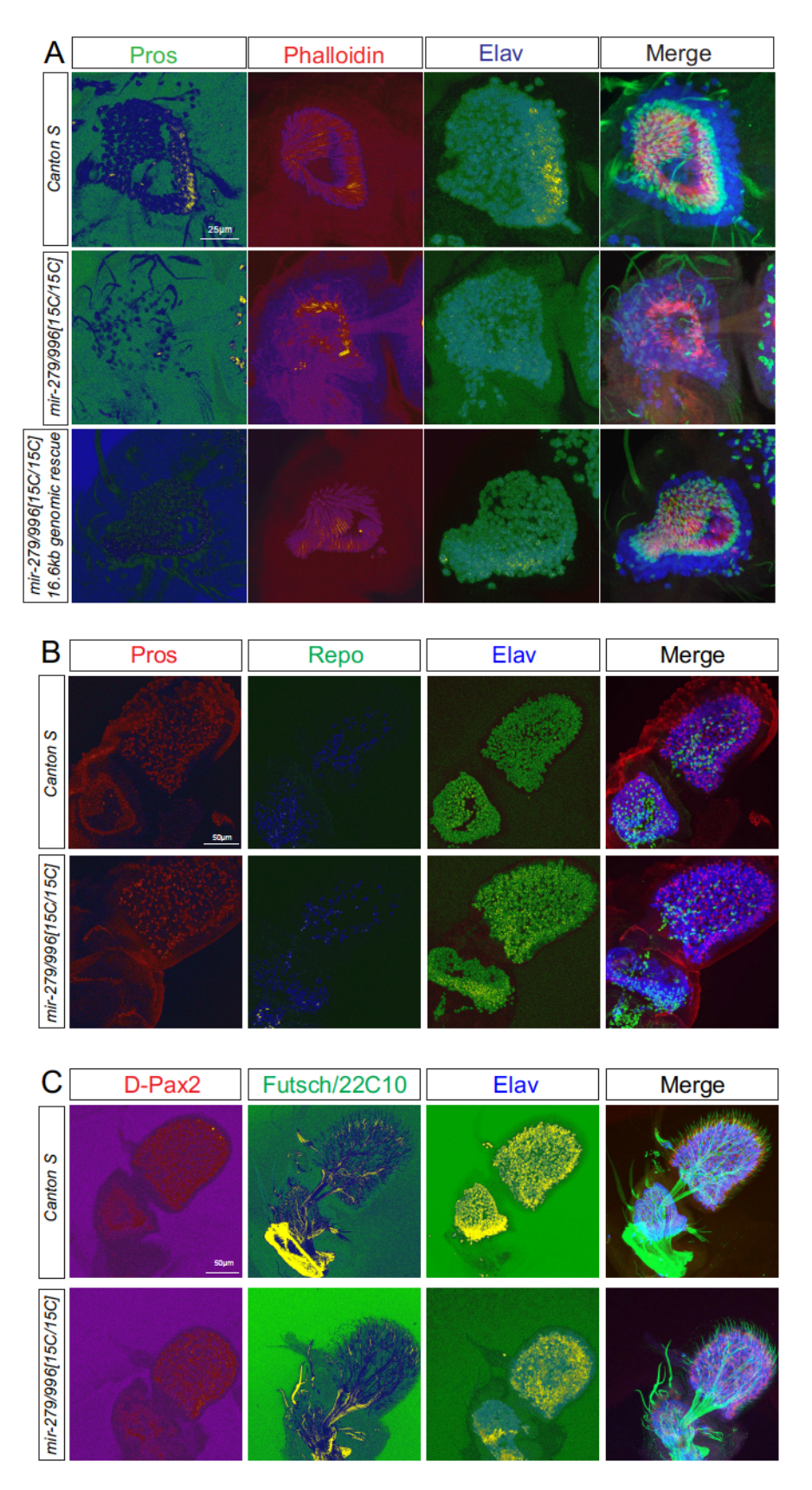
Genes Dev. 2023, 37: originally published online December 18, 2023 Access the most recent version at doi:10.1101/gad.351052.123

Supplemental Material	http://genesdev.cshlp.org/content/suppl/2023/12/18/gad.351052.123.DC1
References	This article cites 81 articles, 19 of which can be accessed free at: http://genesdev.cshlp.org/content/37/21-24/1041.full.html#ref-list-1
Creative Commons License	This article is distributed exclusively by Cold Spring Harbor Laboratory Press for the first six months after the full-issue publication date (see http://genesdev.cshlp.org/site/misc/terms.xhtml). After six months, it is available under a Creative Commons License (Attribution-NonCommercial 4.0 International), as described at http://creativecommons.org/licenses/by-nc/4.0/ .
Email Alerting Service	Receive free email alerts when new articles cite this article - sign up in the box at the top right corner of the article or click here.

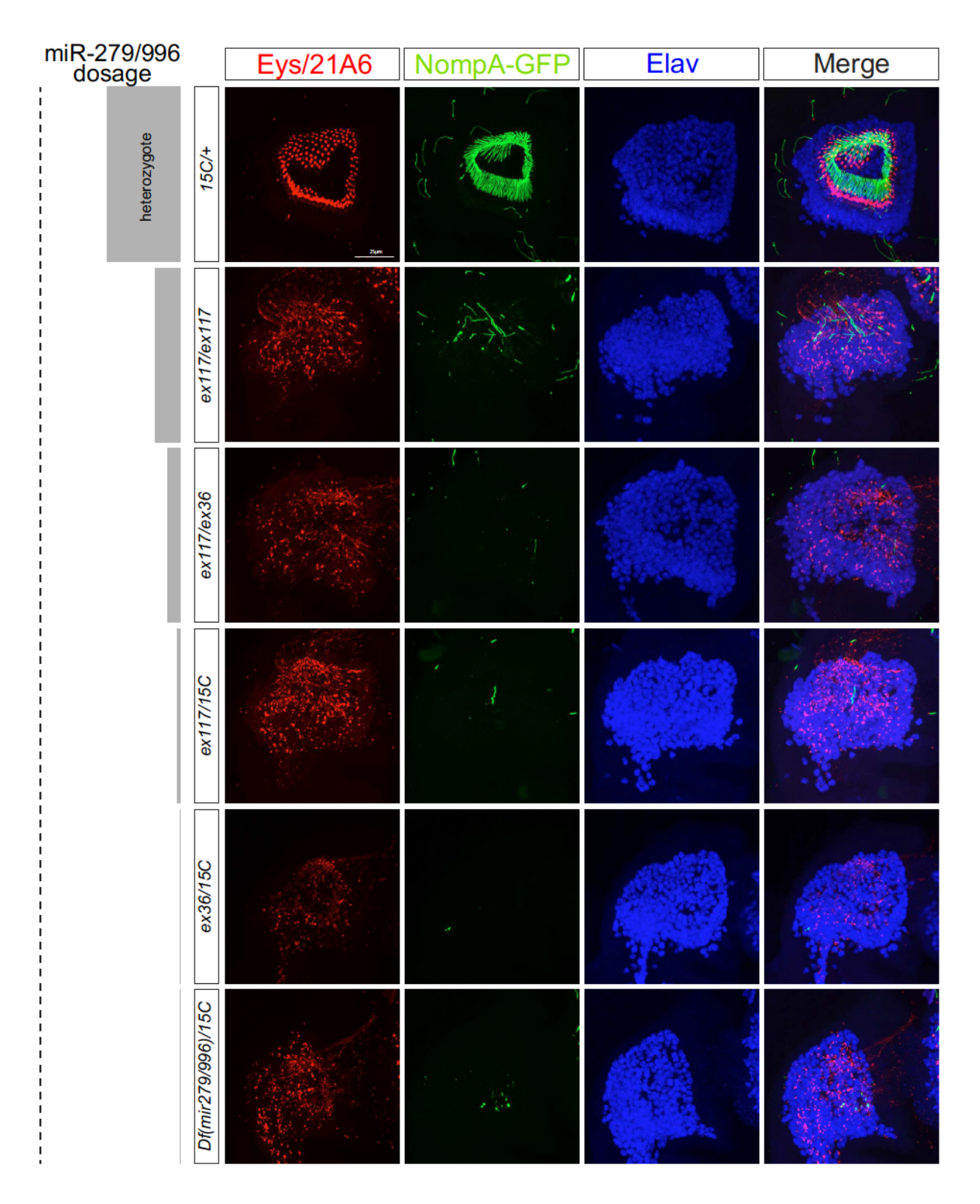
Doing science doesn't have to be wasteful.



Supplementary Figure 1. Analysis of Johnston's organ phenotypes across multiple allelic combinations of *mir-279/996* mutants. Shown are antennae collected at 45 hr after puparium formation, stained for the scolopale marker Pros (in green), the scolopale and cap cell marker D-Pax2 (in red), and the neuronal marker Elav (in blue). The *[ex117]* allele is deleted for *mir-279* and expresses ~5% the normal level of mature miR-996. The *[ex36]* allele is deleted for *mir-279* and does not detectably express mature miR-996. The *[15C]* allele is fully deleted for both *mir-279* and *mir-996*. The allelic combinations tested comprise hypomorphic to null states for *mir-279/996*. All of them selectively disrupt the specification of scolopale cells, with weaker effects in *[ex117]* homozygotes and nearly complete loss of scolopales in all other genotypes tested.

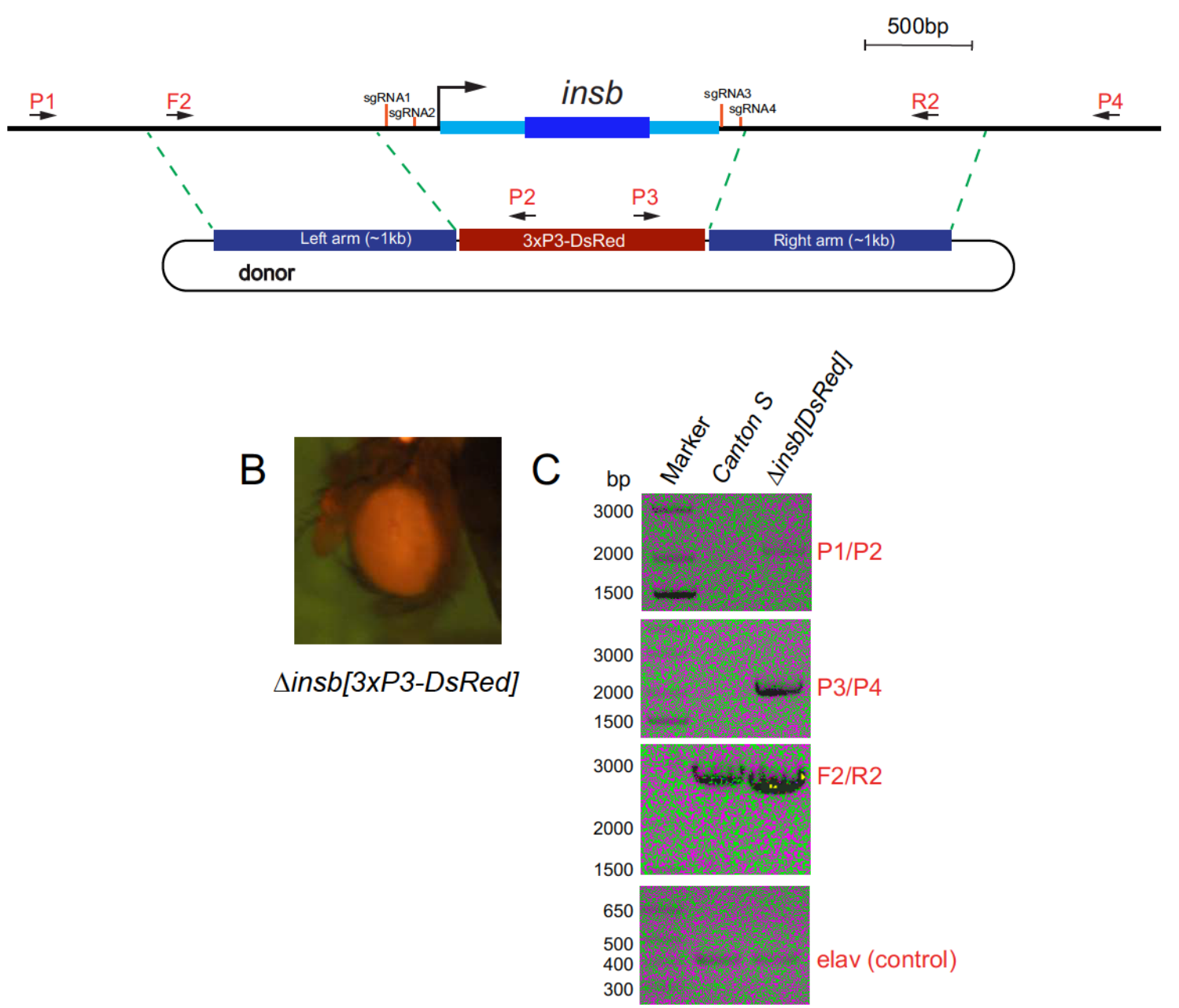


Supplementary Figure 2. Additional analysis of cell markers in *mir-279/996* mutant Johnston's organ (JO). Shown are antennae collected at 45 hr after puparium formation, stained for the indicated markers. *Canton S* is used as a wildtype control. (A) Phalloidin marks scolopale rods, and exhibits highly reduced reactivity in [15C] null JO. The normal pattern of these markers is restored by introduction of a 16.6kb *mir-279/996* genomic rescue transgene. (B) Triple stainings for scolopale marker Pros, glial marker Repo, and neuronal marker Elav. Pros is selectively lost from [15C] null JO, but glial cells remain. (C) Triple stainings for scolopale/cap cell marker D-Pax2, the neuronal membrane marker Futsch/22C10, and the neuronal marker Elav. Despite disorganization, differentiated neurons are evident in [15C] null JO.

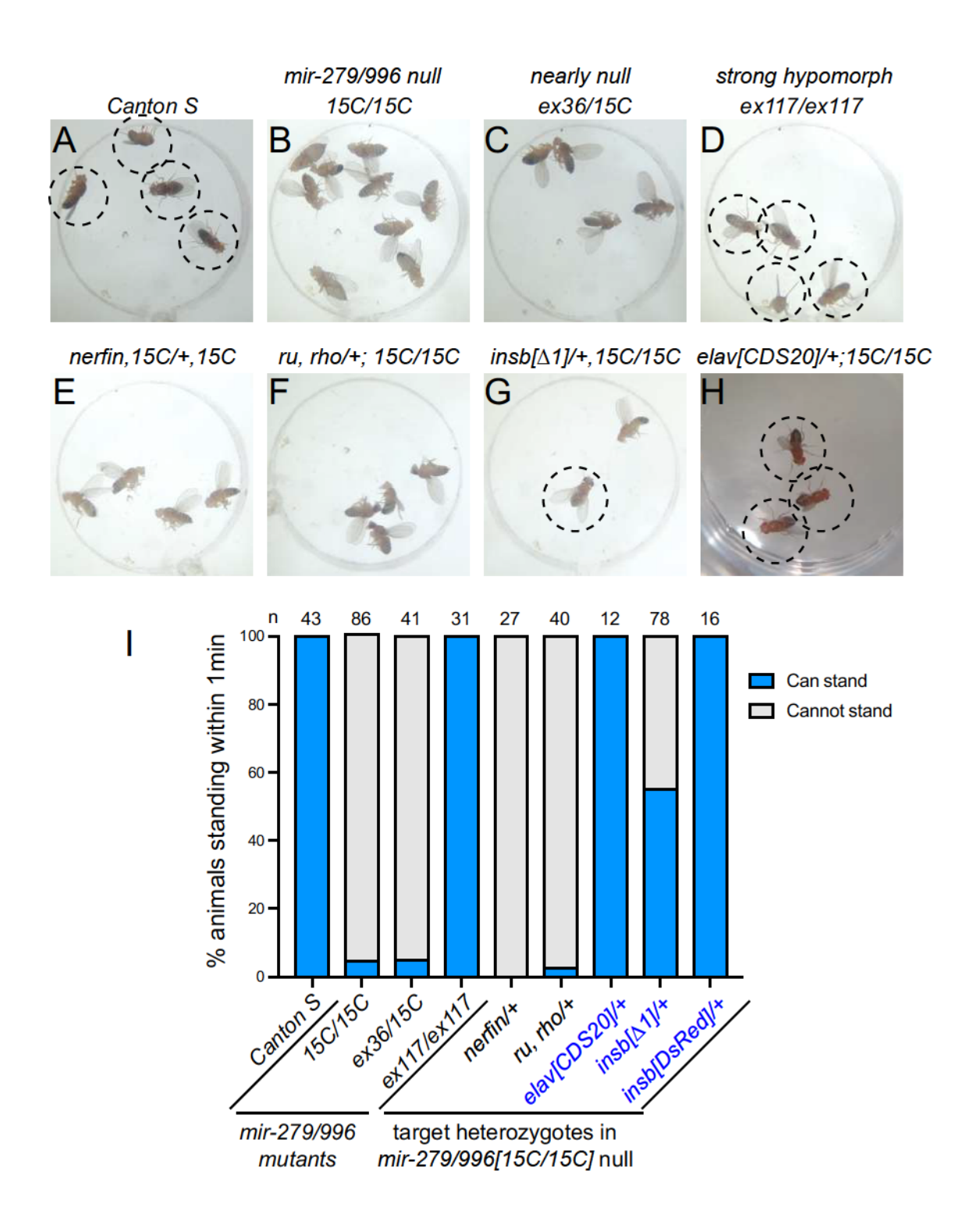


Supplementary Figure 3. Analysis of scolopale differentiation across multiple allelic combinations of *mir*-279/996 mutants. Shown are antennae collected at 45 hr after puparium formation, stained for the scolopale space ECM marker 21A6 (red), the dendritic cap marker NompA-GFP (green), and the neuronal marker Elav (blue). The heterozygote of the *mir*-279/996[15C] deletion allele is used as a control (50% dosage); this genetic situation is morphologically wildtype. The [ex117] allele is deleted for *mir*-279 and expresses ~5% the normal level of mature miR-996. The [ex36] allele is deleted for *mir*-279 and does not detectably express mature miR-996. The allelic combinations tested comprise hypomorphic to null states for *mir*-279/996. All of them selectively disrupt the differentiation of scolopale cells, with strong defects observed in hypomorphic and null conditions alike.

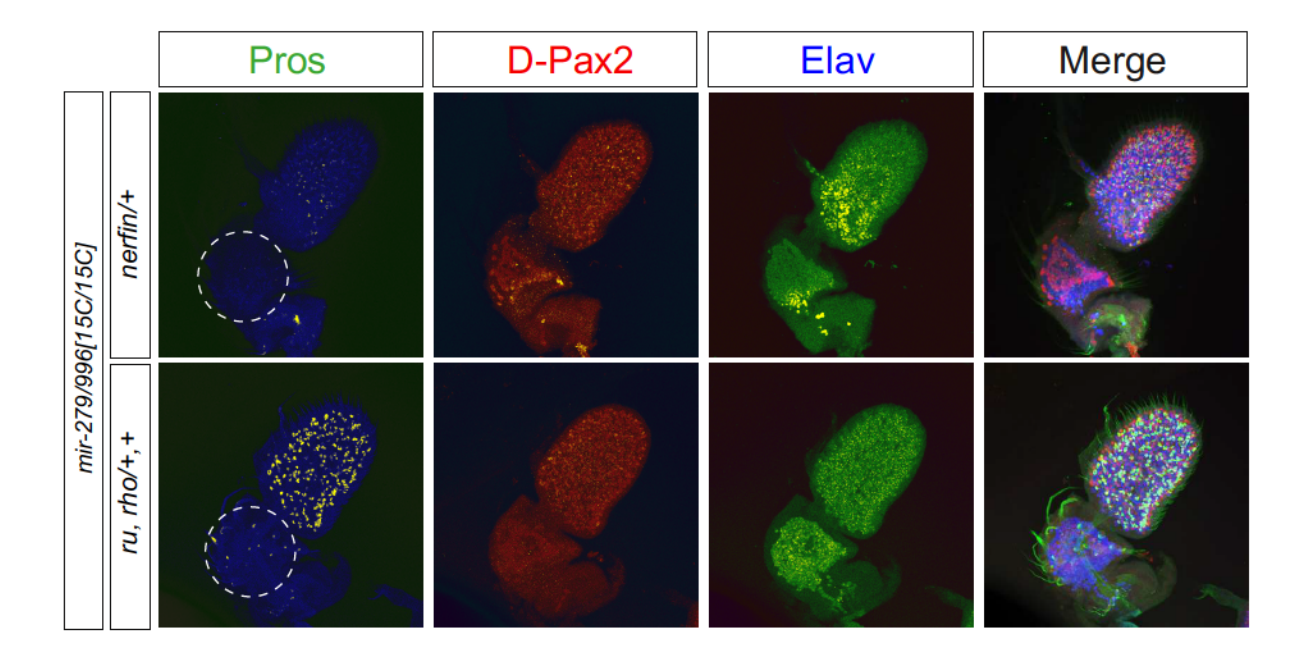
A D. melanogaster insb CRISPR deletion strategy



Supplementary Figure 4. CRISPR/Cas9-mediated deletion of the insensible (insb) locus. (A) We injected multiple gRNAs and an HDR donor vector into nos-Cas9 embryos, and screened for replacement of insb with 3xP3-DsRed. (B) Example knockin event showing DsRed fluorescence in the eye. (C) PCR validation of on-target insertion of DsRed and deletion of *insb*.



Supplementary Figure 5. Suppression of gross postural defects in *mir-279/996* mutants by specific target mutants. (A-H) Capacity of different fly genotypes to stand. (A) All wildtype flies (Canton S used here) stand readily. (B-C) Null or nearly-null conditions of *mir-279/996* render most animals unable to stand, and they are mostly on their sides or back. (D) Strong hypomorph of *mir-279/996* is compatible with standing, but not normal locomotion. (E-H) Effect of miR-279/996 target heterozygosity on *mir-279/996[15C/15C]* null behavior. (E) *nerfin/+* and (F) *ru*, *rho/+*, + conditions do not improve standing behavior in mutants, even though these genetic backgrounds suppress *mir-279/996[15C/15C]* mutant defects in CO2 sensing neurons and in eye development, respectively. (G) *insb/+* restores standing behavior in 15C/15C mutants, as does *elav/+* (H). (I) Quantification of flies that stood within 1 min assay.



Supplementary Figure 6. Control genetic interaction tests of target mutants that do not modify Δ*mir*-279/996 JO defects. Previous studies showed that heterozygosity for nerfin (Cayirlioglu, Science 2008) or double heterozygosity for ru and rho (Duan, Development 2018) can rescue defects of Δ*mir*-279/996 mutants in the olfactory system or the eye, respectively. However, these target heterozygous backgrounds do not rescue loss of Pros+ cells in the Johnston's organ (dotted circles) in Δ*mir*-279/996 mutants.

Primer name	sequence	purpose
mir-279-F	CAAGAAACCACCCCGAGAAGAAGAAG	mir-279/996 mutant allele genotyping
mir-279-R	AGCAGGTGTTACAGTTACACTCAAACG	mir-279/996 mutant allele genotyping
U6-seq-F	ACGTTTTATAACTTATGCCCCTAAG	Amplify and sequence multiple guide RNAs cloned in pCFD5
pCFD-seq-R	GCACAATTGTCTAGAATGCATAC	Amplify and sequence multiple guide RNAs cloned in pCFD5
elavCDS20-F	CAGCAACAACAGCAGGCG	elav5 or elavCDS20 mutant allele genotyping
elavCDS20-R	ACAATAAGGTTTGTGCGCGTC	elav5 or elavCDS20 mutant allele genotyping
nsb PCR 1F	GCGGCCCGGGTTCGATTCCCGGCCGATGCAGTGTCCGTTTCCTTTCGGTGGTTTTAGAGCTAGAAATAGCAA	
nsb PCR 1R	ATTCCCAAGTTACCTTCCTACTGCACCAGCCGGGAATCGAACCCG	pCFD5-insb-guide
nsb PCR 2F	GTAGGAAGGTAACTTGGGAATGTTTTAGAGCTAGAAATAGCAAG	pCFD5-insb-guide
nsb PCR 2R	CTTCCTTTATGTTTTACTTTCTGCACCAGCCGGGAATCGAACCC	pCFD5-insb-quide
nsb PCR 3F	GAAAGTAAAACATAAAGGAAGGTTTTAGAGCTAGAAATAGCAAG	pCFD5-insb-guide
nsb_PCR_3R:	ATTTTAACTTGCTATTTCTAGCTCTAAAACAGCTAGGATGGAACCCCCCACTGCACCAGCCGGGAATCGAACCC	pCFD5-insb-guide
HR1F-Aarl	ATATATCACCTGCTTCATCGCGGGACAGGAGATTCTTCA	primer design for homology arm Aarl
HR1R-Aarl	ATATATCACCTGCGATCCTACCCCAAGTTACCTTCCTATG	primer design for homology arm Aarl
HR2F-Sapl	ATATATGCTCTTATGCTGGGAATAAAAAAACACTC	primer design for homology arm Sapl
HR2R-Sapl	ATATATGCTCTTCCGACGCGTATGAATAACAAATACTCC	primer design for homology arm Sapl
HR1-GT-F	TGAACATTATCGCGAGCC	Clone validation primers
HR1-GT-R	GCGCCTCTATTTATACTCC	Clone validation primers
HR2-GT-F	CACTGCATTCTAGTTGTGG	Clone validation primers
HR2-GT-R	TTTTGTGTCGCCCTTGAAC	Clone validation primers
P1	GTCGCGTGCTTCTCAAACTG	PCR verification of insb[attp-Dsred] mutant
P2	GATGTCCCAGGCGAAGGGCAGGG	PCR verification of insb[attp-Dsred] mutant
23	ATCTACATGGCCAAGAAGCCC	PCR verification of insb[attp-Dsred] mutant
24	GAGCTGTATTCGGTCGGGAG	PCR verification of insb[attp-Dsred] mutant
Elav-F	TAAACGACAACGAAACGGCG	Control elav
Elav-R	TGGAAGATTTCATTGCTGCG	Control elav
F2	CTCCATGCCAACGGAGGTAA	PCR verification of insb[attp-Dsred] mutant
R2	GATTCGGAGGGATGGATGG	PCR verification of insb[attp-Dsred] mutant